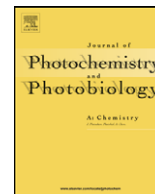




Contents lists available at ScienceDirect

Journal of Photochemistry and Photobiology A: Chemistry

journal homepage: www.elsevier.com/locate/jphotochem

Study of alloxymidim photodegradation in the presence of natural substances: Elucidation of transformation products

Beatriz Sevilla-Morán^a, Pilar Sandín-España^a, M. Jesús Vicente-Arana^b,
José L. Alonso-Prados^a, José M. García-Baudín^{a,*}

^a Departamento de Protección Vegetal, Instituto Nacional de Investigación y Tecnología Agraria y Alimentaria (INIA),
Ctra. de La Coruña, Km. 7.5, 28040 Madrid, Spain

^b Servicio Interdepartamental de Investigación, Universidad Autónoma de Madrid,
Campus de Cantoblanco, 28049 Madrid, Spain

ARTICLE INFO

Article history:

Received 28 November 2007
Received in revised form 6 March 2008
Accepted 10 March 2008
Available online 16 March 2008

Keywords:

Photodegradation
Alloxymidim
Time-of-flight mass analyser
Aqueous solution
Natural substances

ABSTRACT

A photodegradation study of alloxymidim was performed under simulate solar irradiation (Suntest apparatus) at different irradiation intensities. Moreover, indirect photolysis of the tested herbicide was investigated under the presence of various concentrations of humic acids (HA), nitrate and Fe (III) ions. The photodegradation of alloxymidim follows a first-order reaction kinetics in all cases. HA inhibited the photolysis kinetic whereas rate constants measured in the presence of nitrate ions indicated no effect on degradation. On the contrary, Fe (III) ions enhanced the photodegradation rate of alloxymidim. Kinetics experiments were monitored by HPLC–DAD and the half-lives ranged from 165.78 to 4.63 min for different intensities in direct photolysis and from 104.81 to 1.14 min for indirect photolysis. The study of transformation products have been investigated by HPLC coupled to quadrupole time-of-flight mass spectrometry (QTOF-MS) employing the electrospray technique.

The most important transformation process was found to be the cleavage of the O–N bond of the oxime moiety. Minor photo-isomerization to Z-isomer was also observed. The appearance of these degradation products is reported in aqueous media for the first time.

© 2008 Elsevier B.V. All rights reserved.

1. Introduction

Alloxymidim (Fig. 1) has been developed by BASF AG for post-emergence control of grass weeds and volunteer cereals in sugar beet, vegetables and broad-leaved crops and it is applied at doses between 0.5 and 1.0 kg a.s./ha. Alloxymidim is a selective systemic herbicide from the cyclohexanedione oxime class. This family of compounds has been developed during the last 30 years as post-emergence herbicides that inhibit acetyl-CoA carboxylase [1,2], the enzyme that catalyses fatty acid synthesis. The cyclohexanedione ring and the ethoxyimine group linked to ring position 3 seem to be essential for the phytotoxic activity, whereas substitutions in position 6 may vary considerably without large differences on herbicidal activity [1].

One common degradation process of these compounds in aqueous media is photochemical degradation. For this to occur in

water, the emission spectrum of the sun needs to fit the adsorption spectrum of the pollutant. However, when the pesticide does not absorb solar light, its transformation can be photoinduced by different absorbing species, present or added in the aqueous medium (HA [3–5], nitrate ions [5,6], or Fe (III) aquacomplexes [7]).

Determination of degradation products (DPs) of organic compounds is nowadays one of the major challenges in analytical chemistry of environmental pollutants. DPs are often more toxic [3,8] and/or persistent [9] in environmental matrices than their parent. On the other hand, their identification is rather difficult due to the limited knowledge about their composition. Their detection is complicated by their generally low ($\mu\text{g/l}$) concentrations, polar character, thermolability and unknown kinetics of degradation reactions.

It has been demonstrated that the use of different light sources (natural sunlight, mercury and xenon arc lamps) under identical aqueous conditions, produces similar degradation products, the only difference being the kinetics of formation [10]. Natural sunlight photodegradation processes are usually compared with those obtained under controlled conditions, generally using a xenon

* Corresponding author. Tel.: +34 91 347 68 40; fax: +34 91 347 14 79.
E-mail address: baudin@inia.es (J.M. García-Baudín).

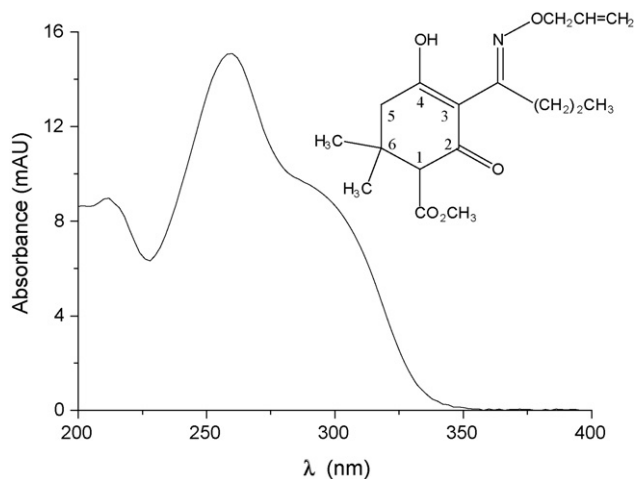


Fig. 1. UV absorption spectrum of alloxymid.

arc lamp [11,12]. This light source fit the solar radiation spectrum best over the whole range of spectral emission [13]. These studies allow the modelling of pesticide behaviour after its application, in order to obtain information about the degradation kinetic and half-life and to increase the information available about the degradation products that can be formed under natural conditions.

The irradiation energy is an important factor to be taken into account, because the photoproduct's final concentrations may change depending on it [14].

An increasing presence of medium and highly polar pollutants in aqueous samples has already favoured the use of liquid chromatography. Among the detection systems available for the HPLC methods [15], ESI-QTOF-MS offers the possibility of analyzing low and high molecular weight compounds with a soft ionization method, good reproducibility and high sensitivity [16], and the possibility to isolate precursor ions for further analysis by tandem mass spectrometry (MS/MS) with the high efficiency, sensitivity and accuracy of a TOF mass analyser across the full mass range [17].

Whereas the degradation of many herbicides in aqueous media has been widely studied [4], few data concerning degradation of cyclohexanedione herbicides in aquatic environment are available. In previous works of our group, the rapid degradation suffered by the herbicide tepraloxymid, alloxymid and clethodim in chlorinated water was reported [18–20].

Hashimoto et al., observed that the main photoproducts of alloxymid on soybean plants were imine and two isomeric oxazoles of alloxymid [21]. Similar results were obtained by Soeda et al., in acetone solution, on TLC plate and on sugar beet plants [22]. Ono et al., observed the photodegradation of alloxymid in soil under natural sunlight to imine, two isomeric oxazoles of alloxymid, and other by-products [23].

The objectives of this work were: (i) to determine the photodegradation kinetic of alloxymid in pure water under different irradiation energies by using xenon arc lamp; (ii) to study the effect of HA, nitrate and Fe (III) ions on the photodegradation rate; and (iii) to detect transformation products formed by photolysis by means of HPLC-ESI-QTOF-MS.

To the best of our knowledge this is the first time that the aqueous photodegradation of herbicide alloxymid has been studied under laboratory conditions.

2. Materials and methods

2.1. Chemicals

All chemical products were used as received. Alloxymid (methyl (*E*)-(RS)-3-[1-(allyloxyimino)butyl]-4-hydroxy-6,6-dimethyl-2-oxocyclohex-3-enecarboxylate) was obtained from Dr. Ehrenstorfer GmbH (Augsburg, Germany) as the sodium salt (98% purity, pK_a 3.7 and 2 kg/l solubility in water). Humic acid sodium salt (technical grade) was purchased from Aldrich (Steinheim, Germany). Potassium nitrate (suprapur) and formic acid (p.a.) was purchased from Merck (Damstadt, Germany). Iron (III) perchlorate hexahydrate (reagent grade) was purchase from Alfa Aesar GmbH (Karlsruhe, Germany).

Acetonitrile (HPLC far UV grade) and isopropanol (HPLC grade) were obtained from Labsan (Stillorgan, Co., Dublin, Ireland). The water used for LC mobile phase and aqueous solutions was purified with a Millipore system (Milli-Q-50 18 m Ω).

Stock solution of alloxymid (50 mg/l) were prepared in milli-Q water and stored at 4 °C in dark without previous degassing. These solutions were used to prepare more dilute standard solutions (5 mg/l). Stability of stock and standard solutions under these conditions was checked and demonstrated for at least 2 months.

2.2. LC analysis

Photodegradation kinetics were performed with a HPLC system (series 1100; Agilent Technologies, Palo Alto, CA, USA) coupled to a photodiode array detector (DAD). The analytical column used was a Waters Nova-Pak[®] C₁₈ column (4 μ m particle size, 3.9 mm \times 150 mm) with a ODS precolumn and were maintained at 25 °C. The mobile-phase was a mixture of water acidified with 0.1% of formic acid (A) and acetonitrile (B). The following gradient was used: 50% B for 1.2 min, linear increase of B to 60% in 0.8 min, then increase of B to 70% in 1 min and this composition was held for 4 min. The flow rate was 1 ml/min and the injection volume was 20 μ l.

For the identification of by-products mass spectrometry experiments were performed HPLC system (series 1100; Agilent Technologies, Palo Alto, CA, USA) coupled to a hybrid QTOF mass spectrometer (QStar Pulsar I, Applied Biosystems). Just before the separation, an external calibration in the mass spectrometer was performed with a mixture of phosphazenes. The experiments were performed in positive ion mode. The instrumental parameters were set as follows—mass range analysed: 50–1200; ion spray voltage (IS): 5000 V; ion source gas pressure (GS1): 65 psi; ion source gas 2 (GS2): 65 psi; curtain gas pressure (Cur): 20 psi; declustering potential (DP): 70 V; focusing potential (FP): 250 V; declustering potential 2: 15 V.

In MS/MS experiments the collision energy (CE) for each ion selected was kept at 22 eV. The column, precolumn, mobile phase and gradient employed were the same as previously described except the flow rate that was 0.7 ml/min. In order to identify as many by-products as possible degradation experiments were carried out with an initial concentration of alloxymid of 80 mg/l.

2.3. Photodegradation experiments

Photochemical experiments were conducted in a Suntest CPS+ apparatus from Atlas (Linsengericht, Germany) equipped with a xenon arc lamp (1500 W) and Special UV Glass (Suprax) filter restricting the transmission of wavelength below 290 nm. The aqueous solutions (20 ml) of alloxymid, prepared at 5 mg/l in milli-Q water, were exposed to simulated solar irradiation in capped cylindrical quartz cuvettes with magnetic stirring. Direct

Table 1
Kinetic parameters of alloxymid photolysis at different light intensities under simulated solar irradiation

Light intensity (W/m ²)	k_{phot} ($\times 10^{-3} \text{ min}^{-1}$)	$t_{1/2}$ (min)	R^2
250	4.19 a \pm 0.06	165.78 \pm 0.16	0.999
500	9.19 b \pm 0.19	75.45 \pm 0.15	0.999
750	17.08 c \pm 0.68	40.63 \pm 0.22	0.998

Different letters show significant differences according to least significant differences (LSDs) test at a significance level of 95%.

photodegradation kinetics experiments were carried out at different irradiation intensities of 250, 500 and 750 W/m² maintained throughout the experiments measured by internal radiometer. A Suncool chiller was used to maintain a mean internal temperature of $25 \pm 1^\circ \text{C}$.

In order to study indirect photodegradation kinetics, experiments were conducted in the same quartz cuvettes and initial concentration of alloxymid and in the presence of substances that can be found in natural waters such as HA, nitrate and Fe (III) ions at various concentrations (0.5–20 mg/l) [8,24,25]. All the solutions were filtered through a 0.2 μm membrane filter prior to injection.

Meanwhile, control experiments in the dark (blank experiments) under the same conditions and initial concentrations of alloxymid and natural substances were carried out in parallel for comparison without the application of light. For all degradation kinetics studies, each experiment was conducted in triplicate and carried out until disappearance of the herbicide was achieved. At selected time intervals, samples were collected and quantitatively analysed directly by HPLC–DAD for the amount of the compound of interest remaining in solution after irradiation based on external calibration.

2.4. Analysis of data

The rate of disappearance of alloxymid follows a first-order kinetics given by the equation:

$$C_t = C_0 e^{-kt}$$

where C_0 and C_t are the concentrations at times 0 and t , t is the irradiation time and k is the first-order rate constant. The fitting of the experimental data was satisfactory for all the samples.

The half-life $t_{1/2}$ of alloxymid, the time required for its concentration to fall to half its initial value, is related to the rate constant by the equation: $t_{1/2} = \ln 2/k$.

Table 2
ANOVA results of light intensity and different concentrations of natural substances at a significance level of 95%

Source of variation	SS ^a	d.f. ^b	MS ^c	F-test	p-Value ^d
Light intensity	2.6756×10^{-4}	2	1.3378×10^{-4}	1679.47	0.0000
Error	4.7793×10^{-7}	6	7.9656×10^{-8}		
Total	2.6804×10^{-4}	8			
Concentration HA	1.3691×10^{-4}	4	3.4227×10^{-5}	460.62	0.0000
Error	7.4307×10^{-7}	10	7.4307×10^{-8}		
Total	1.3765×10^{-4}	14			
Concentration nitrate	2.6279×10^{-6}	4	6.5698×10^{-7}	0.96	0.4701
Error	6.8435×10^{-6}	10	6.8435×10^{-7}		
Total	9.4714×10^{-6}	14			
Concentration Fe (III) ions	6.9541×10^{-1}	4	1.7385×10^{-1}	744.00	0.0000
Error	2.3367×10^{-3}	10	2.3367×10^{-4}		
Total	6.9774×10^{-1}	14			

^a Sum of squares.

^b Degrees of freedom.

^c Mean squares.

^d Critical value of F.

Table 3
Kinetics parameters of alloxymid in the presence of various concentrations of natural substances

Substance	Concentration (mg/l)	k_{phot} ($\times 10^{-3} \text{ min}^{-1}$)	$t_{1/2}$ (min)	R^2
HA	1	15.16 a \pm 0.25	45.76 \pm 0.09	0.999
	5	11.05 b \pm 0.22	62.79 \pm 0.13	0.999
	10	8.98 c \pm 0.21	77.27 \pm 0.17	0.998
	15	7.40 d \pm 0.15	93.77 \pm 0.16	0.999
	20	6.62 e \pm 0.17	104.81 \pm 0.23	0.997
Nitrate ions	1	16.90 a \pm 0.28	41.06 \pm 0.09	0.999
	5	17.02 a \pm 0.44	40.76 \pm 0.14	0.999
	10	16.87 a \pm 0.25	41.11 \pm 0.08	0.999
	15	17.12 a \pm 0.57	40.49 \pm 0.17	0.997
	20	17.27 a \pm 0.31	40.15 \pm 0.09	0.998
Fe (III) ions	0.5	42.32 a \pm 5.62	16.39 \pm 0.45	0.986
	1	77.19 b \pm 10.92	8.98 \pm 0.35	0.980
	2.5	223.73 c \pm 4.87	3.10 \pm 0.03	0.999
	5	434.38 d \pm 20.51	1.60 \pm 0.05	0.997
	10	607.45 e \pm 38.10	1.14 \pm 0.06	0.997

Different letters show significant differences according to least significant differences (LSDs) test at a significance level of 95%.

One-way analyses of variance (ANOVA) were conducted to determine differences between intensities and between concentrations of natural substances, at the 0.05 significance level. Results were analysed using a statistical procedure (Statgraphics Plus 4.1[®]).

3. Results and discussion

3.1. Phototransformation kinetics

Alloxymid showed a maximum absorbance at $\lambda = 260 \text{ nm}$ and a shoulder about 292 nm in aqueous solution (Fig. 1). Spectral data indicated that alloxymid absorbed light at wavelengths over 290 nm and therefore being capable of absorbing the UV energy of light. This fact suggests that natural sunlight could be responsible for the direct phototransformation of alloxymid in aquatic environments.

Alloxymid was irradiated in milli-Q water under different light intensities. The initial mass concentration of alloxymid was 5 mg/l. This concentration was selected to ensure the identification of alloxymid by-products produced during degradation.

The photodegradation kinetic of alloxymid disappearance was of first-order in all cases. The net first-order rate constants (k_{phot})

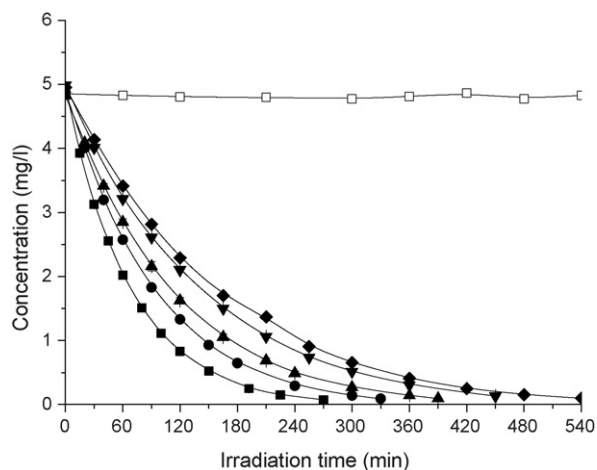


Fig. 2. Photodegradation of alloxylim in various concentrations of HA in milli-Q water under simulated solar irradiation: (■) [HA] = 1 ppm; (●) [HA] = 5 ppm; (▲) [HA] = 10 ppm; (▼) [HA] = 15 ppm; (◆) [HA] = 20 ppm; (□) blank experiment.

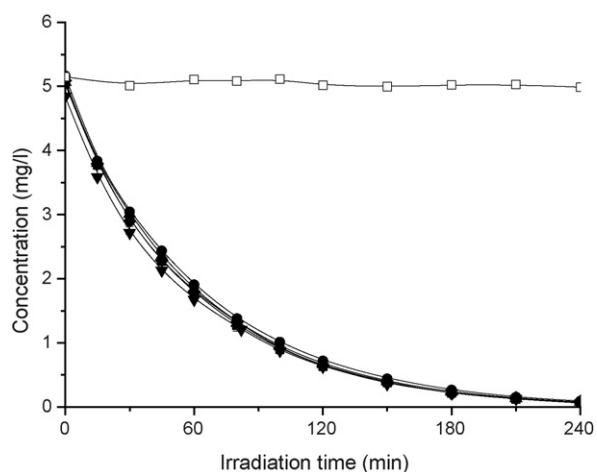


Fig. 3. Photodegradation of alloxylim in various concentrations of nitrate in milli-Q water under simulated solar irradiation: (■) [nitrate] = 1 ppm; (●) [nitrate] = 5 ppm; (▲) [nitrate] = 10 ppm; (▼) [nitrate] = 15 ppm; (◆) [nitrate] = 20 ppm; (□) blank experiment.

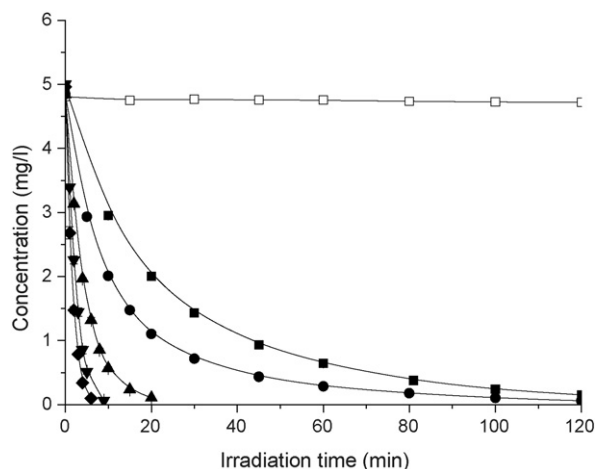


Fig. 4. Photodegradation of alloxylim in various concentrations of Fe (III) ions in milli-Q water under simulated solar irradiation: (■) [Fe (III)] = 0.5 ppm; (●) [Fe (III)] = 1 ppm; (▲) [Fe (III)] = 2.5 ppm; (▼) [Fe (III)] = 5 ppm; (◆) [Fe (III)] = 10 ppm; (□) blank experiment.

and the half-lives ($t_{1/2}$) for different light intensities are listed in Table 1.

Table 1 shows that alloxylim photodegradation rate was lower at the lowest light intensity following the order: $250 < 500 < 750 \text{ W/m}^2$ illustrating a strong dependence on the intensity of irradiated light. The analysis of variance showed significant differences among the three intensities (Table 2).

Quantitative recoveries from blank experiments sampled over the entire exposure period of simulated solar irradiation showed that alloxylim did not undergo dark reactions (hydrolysis).

The next subject was to investigate indirect photodegradation. For this purpose, experiments with the same initial concentration of alloxylim and various concentrations of HA, nitrate and Fe (III) ions were carried out under simulated solar irradiation.

Non-linear regression of data points to first-order kinetics allowed the calculation of the rate constants and half-lives (Table 3 and Figs. 2–4).

In blank experiments, no modification of the initial concentration of alloxylim was observed. Therefore, the decline observed in the degradation curve must be attributed to a photodegradation process.

One of the primary light-absorbing species in natural waters are HA. Their complex structure is basically composed by phenolic, carbonylic and carboxylic groups. HA are dark brown to black in colour and absorb radiation in the range 300–600 nm. The degradation of organic pollutants that absorb slightly at $\lambda > 280 \text{ nm}$ can be inhibited because HA act as photon trap (“optical filter” effect). However, the degradation can be enhanced by formation of reactive species from HA as hydroxyl radicals, singlet oxygen, solvated electrons, and hydrogen peroxide (“sensitizer” effect) [26–28].

In the case of HA, results showed that photodegradation rate of alloxylim were lower than in milli-Q water, in other words as the HA concentration increases the rate of photolysis decreases (Table 3). Analysis of variance showed significant differences amongst each concentration (Table 2). This showed a strong dependence on the concentration of HA present in the aqueous media.

The diminished rate of alloxylim indicate that HA absorbed most of the photons emitted thereby slowing down direct photochemical reaction of alloxylim (“optical filter” effect).

When comparing the rate constants with HA concentration, the influence was not proportional since a 20-fold increase in HA resulted in only a 12–62% decrease in the reaction rate. Other authors explained these results as a combination of “optical filter” effect coupled with a sensitization effect by the HA due to the generation of hydroxyl radicals [6,29].

Nitrate photolysis, which is a potential source of hydroxyl radicals in natural waters, can initiate rapid reactions leading to the degradation of organic micropollutants [8,30]. In our study, increased nitrate concentrations from 1 to 20 mg/l showed no significant differences neither them nor with milli-Q water (Fig. 3, Tables 2 and 3). Similar results have been obtained by other authors [31,32]. The rate of nitrate ions photolysis depends on the irradiating power available in the solution which can be significantly reduced when the substrate itself strongly absorbs in it same UV range. Therefore, alloxylim could reduce the radiation absorbed by nitrate ions.

Experiments conducted with the same concentration of alloxylim and various concentrations of Fe (III) ions produced first-order degradation curves, allowing the calculation of rate constants. In all cases the presence of Fe (III) ions increased the rate of photolysis (Fig. 4). Analysis of variance showed significant differences among each concentration (Tables 2 and 3).

As largely reported in the literature that the photodegradation of pesticides and other organic compounds is enhanced by the pres-

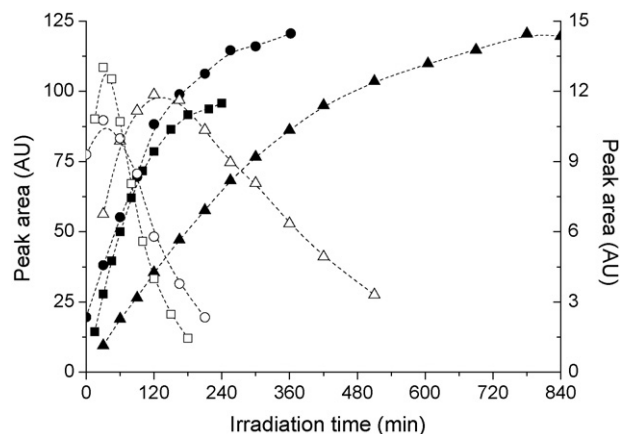


Fig. 5. Evolution of transformation products coming from degradation of alloxylim irradiated at different intensities. Solid symbols refer to A1 product and to the left ordinate: (\blacktriangle) 250 W/m²; (\bullet) 500 W/m²; (\blacksquare) 750 W/m². Open symbols to the right ordinate and correspond to A2 product: (\triangle) 250 W/m²; (\circ) 500 W/m²; (\square) 750 W/m².

ence of aqueous Fe (III) ions in solution [30]. The irradiation of iron (III) aqua complexes at $\lambda > 300$ nm results in the formation of hydroxyl radicals, which can oxidize most organic compounds [33,34]. On the other hand, the organic molecule can form a complex with the Fe (III) ion and later undergoes a direct photolysis [30,35].

In order to check if hydroxyl radicals were involved in the alloxylim degradation, an excess of isopropanol, scavenger of hydroxyl radicals, was added to a solution of Fe (III) ions and HA. The degradation rate of alloxylim was hardly affected by isopropanol, which indicated that hydroxyl radicals were not responsible for alloxylim degradation in the presence of these natural substances.

3.2. Phototransformation products

The disappearance of alloxylim irradiated at 250, 500 and 750 W/m² is achieved in 250, 400 and 850 min, respectively. Concomitantly with the disappearance of alloxylim, the formation of two transformation products A1 and A2 is realized, whose kinetic profiles are reported in Fig. 5. A1 is formed in large amount during alloxylim transformation and reached its maximum concentration when alloxylim is completely disappeared. In the three intensities experiments, a second by-product A2 is formed in smaller amounts. A2 concentration reached maximum levels after irradiation for 30, 35 and 120 min at 250, 500 and 750 W/m² intensities respectively and thereafter slowly dropped to trace levels.

Experiments of indirect photolysis carried out with HA, nitrate and Fe (III) ions showed the same two by-products, A1 and A2. At the same way that direct photolysis, their kinetic profiles have a very

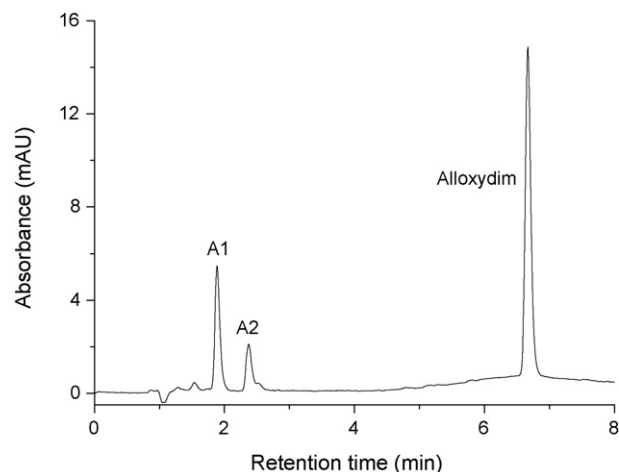


Fig. 7. HPLC-DAD chromatogram of alloxylim photodegradation in milli-Q water.

similar evolution, being A1 the main by-product formed while A2 is only produced in small amounts. A1 reached its maximum amount at the end of the degradation of alloxylim and A2 is produced in the first stages of the degradation and thereafter decline till complete disappearance (data not shown). In the presence of Fe (III) ions A1 is formed in smaller amounts than in the presence of HA and nitrate ions, while by-product A2 is produced in higher amounts. Fig. 6 illustrates the maximum amount of A1 and A2 reached during indirect photodegradation of alloxylim.

A1 and A2 had a retention time of 1.89 and 2.37 min, respectively, showing a more polar character than alloxylim. Typical chromatogram from an irradiated aqueous sample is shown in Fig. 7.

There were no available standards with which to match HPLC-DAD retention times, so by-products were tentatively identified by HPLC-ESI-QTOF.

Accurate mass measurements from all the samples are shown in Table 4 for the protonated molecules, and empirical molecular formulae are also obtained using the elemental composition calculator incorporated in the Software. The different hits for sum formulae based on the accurate masses and the main fragments obtained from the alloxylim MS results are also shown in this table.

E-alloxylim (Fig. 8) has a molecular mass of 323 and a retention time of 7.40 min. The fragment of m/z 266 is formed through the loss of the oxime moiety, and the loss of methanol of the methyl ester leads to a fragment of m/z 234. The ion formed can further release a CO molecule with the formation of a fragment of m/z 206. From this ion a new loss of CO leads to the formation of the ion at m/z 178. Accurate mass measurement gave three hits (Table 5), two of them were discarded since it presents four and five nitrogen atoms. This

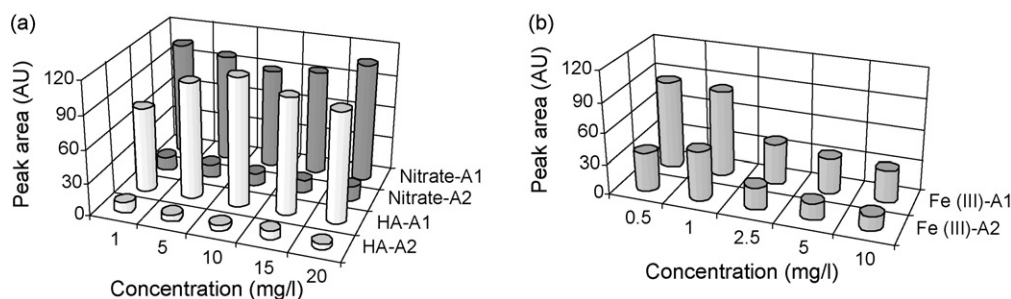


Fig. 6. Maximum amount of by-products A1 and A2 in degradation experiments in the presence of (a) HA, nitrate ions and (b) Fe (III) ions.

Table 4
Fragmentation of *E*-alloxydim, imine and *Z*-alloxydim

Compound	t_R (min)	m/z	Major fragments
<i>E</i> -Alloxydim	7.40	669.3305	$[2M+Na]^+$
		346.1586	$[M+Na]^+$
		324.1798	$[M+H]^+$
		266.1421	$[MH]^+-[HO-CH_2-CH=CH_2]$
		234.1145	$[MH]^+-[HO-CH_2-CH=CH_2-CH_3OH]$
		206.1169	$[MH]^+-[HO-CH_2-CH=CH_2-CH_3OH-CO]$
		178.1225	$[MH]^+-[HO-CH_2-CH=CH_2-CH_3OH-CO-CO]$
Imine	2.86	557.2851	$[2M+Na]^+$
		290.1376	$[M+Na]^+$
		268.1557	$[M+H]^+$
		236.1295	$[MH]^+-[CH_3OH]$
		208.1326	$[MH]^+-[CH_3OH-CO]$
		194.1181	$[MH]^+-[CH_3OH-CH_2=CO]$
		180.1377	$[MH]^+-[CH_3OH-CO-CO]$
<i>Z</i> -Alloxydim	3.60	669.3305	$[2M+Na]^+$
		346.1586	$[M+Na]^+$
		324.1798	$[M+H]^+$
		266.1421	$[MH]^+-[HO-CH_2-CH=CH_2]$
		234.1145	$[MH]^+-[HO-CH_2-CH=CH_2-CH_3OH]$
		206.1169	$[MH]^+-[HO-CH_2-CH=CH_2-CH_3OH-CO]$
		178.1225	$[MH]^+-[HO-CH_2-CH=CH_2-CH_3OH-CO-CO]$

mass measurement was reported with an error of -2.3 ppm, which reflects the performance of the instrument used in this work.

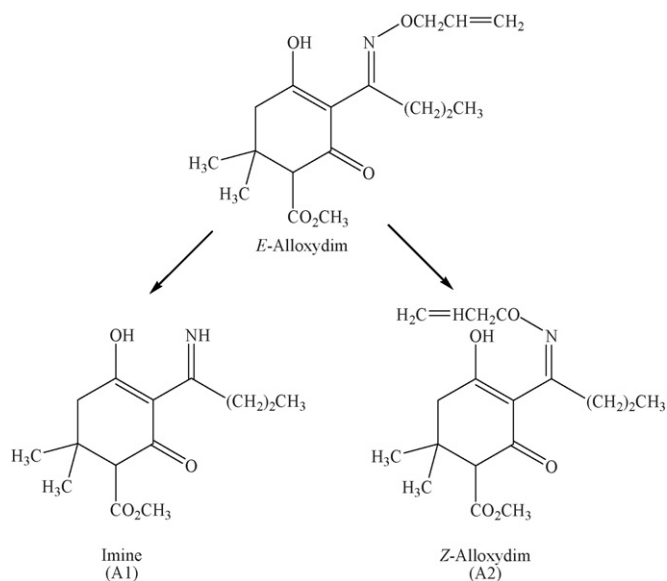
Photoproduct A1 with retention time of 2.86 min is characterized by m/z 268 indicating the molecule contains an odd number of nitrogen atoms, therefore the structure maintained the nitrogen of the oxime moiety. The list of probable molecular composition for this ion indicates that the empirical formula is $C_{14}H_{22}NO_4$ since the other possibilities contain a major number of nitrogens. Comparing the fragments of this by-product with the parent compound, it can be noted that the typical loss of the ether moiety is now absent. Detailed examination of the main fragments in the mass spectrum allowed the identification of this compound as the imine of alloxydim. This photoproduct is characterized by the loss of methanol that leads to a fragment of m/z 236. The ketone formed release a CO molecule with the formation of the fragment 208. From this fragment, a loss of CO leads to the formation of ion at m/z 180. By the other hand from the ion 236, via ketene ($CH_2=CO$) elimination the ion at m/z 194 could be formed.

This by-product has been previously observed as one of the main metabolite in soil, sugar beet and soybean plants [21–23].

The photoproduct A2 presents a retention time shorter than the parent compound (3.60 min), suggesting that the photoproduct is a more polar compound than this active substance (Fig. 7). This compound was detected at m/z 324 leading to a molecular mass of 323. Its mass spectrum gave the same fragments as the parent compound (Table 4) indicating that the photoproduct has the same molecular weight and identical chemical structure. Therefore, the photoproduct A2 has been identified as the *Z*-isomer of alloxydim by isomerization of the oxime moiety. Accurate mass measurement for this degradation product gave four hits (Table 4) and the only one consistent with the number of nitrogen atoms corresponded to the empirical formula of $C_{17}H_{26}NO_5$. In this case, the error was also low enough for the correct identification of degradation product.

Some authors have reported that the oxime isomerization can be induced by temperature, light, acid and/or basic medium and a solvent [36]. Whereas most of the cyclohexanodione herbicides are marketed as the *E*-isomer at the oxime ether double bond, it has been stated that some of them may equilibrate with the *Z*-, *E*-isomer in a polar medium such as water [18,37] or in chlorinated water [19].

It is important to note in Table 5 the double-bond equivalent (DBE) values. For *E*- and *Z*-alloxydim the DBE value was 5.5 and for imine 4.5 as expected, thus adding more confidence to the confirmation of the chemical structures.

**Fig. 8.** Proposed photodegradation pathway of alloxydim in aqueous solution.**Table 5**
Accurate mass measurements for the $[M+H]^+$ ions of alloxydim and degradation products by HPLC-ESI-QTOF-MS

Input m/z	Calculated mass	Error (mDa)	Error (ppm)	DBE	Formula
324.1798	324.1792	0.6	1.8	6.0	$C_{15}H_{24}N_4O_4$
324.1798	324.1805	-0.7	-2.3	5.5	$C_{17}H_{26}NO_5$
324.1798	324.1818	-2.0	-6.4	10.5	$C_{18}H_{22}N_5O$
268.1557	268.1556	0.1	0.1	9.5	$C_{15}H_{18}N_5$
268.1557	268.1570	-1.3	-4.9	9.0	$C_{17}H_{20}N_2O$
268.1557	268.1543	1.4	5.1	4.5	$C_{14}H_{22}NO_4$
324.1814	324.1818	-0.5	-1.5	10.5	$C_{18}H_{22}N_5O$
324.1814	324.1805	0.9	2.6	5.5	$C_{17}H_{26}NO_5$
324.1814	324.1832	-1.8	-5.6	10.0	$C_{20}H_{24}N_2O_2$
324.1814	324.1792	2.2	6.8	6.0	$C_{15}H_{24}N_4O_4$

The chosen best-fit assignments are shown in bold font.

Fig. 8 shows a tentative and simple scheme of the photolysis of *E*-aloxymidim in aqueous samples. The major degradation pathway is the cleavage of the N–O bond [38,39], since this covalent bond is relatively weak (bond dissociation energy of ca. 53 kcal/mol), leading to the imine structure. The other degradation pathway observed was the isomerization of the oxime moiety of aloxymidim.

4. Conclusions

In this study, the photochemical behaviour of aloxymidim in aqueous samples has been investigated. The results demonstrated that degradation rate in direct photolysis was higher as the irradiation intensities was increased. Irradiation of aqueous aloxymidim solutions containing HA substance slowed down the rate of the photodegradation, suggesting the strong filter effect. The presence of nitrate ions had no effect in the degradation rate. On the other hand, Fe (III) ions accelerated the photolysis reaction. In all cases, first-order kinetics was observed.

The photochemical transformation of aloxymidim proceeds through two main pathways, the degradation to the predominant species imine and the photoisomerization to the *Z*-isomer of aloxymidim. Both degradation products are more polar than active substance what could make them easily leach to groundwater and potentially contaminate drinking water sources.

In this study, we have shown the power of time-of-flight mass spectrometry from the chemical elucidation of the photodegradation products of aloxymidim. Accurate mass measurements were obtained for both degradation products and empirical molecular formulae were proposed, thus enhancing the knowledge of the photolysis by-products of aloxymidim.

Acknowledgements

This research has been financed by the CICYT (project AGL2004-05124) project. B.S.-M. has been supported by an INIA predoctoral fellowship. The authors thank Miguelina M. Mateo for its helpful support to the manuscript.

References

- [1] H.K. Lichtenthaler, *Z. Naturforsch.* C 45 (1990) 521–528.
- [2] B.J. Ingleton, J.C. Hall, *Pesticide Biochem. Physiol.* 57 (1997) 255–271.
- [3] E.M. Thurman, M. Meyer, M. Pomes, C.A. Perry, A.P. Schwab, *Anal. Chem.* 62 (1990) 2043–2048.
- [4] V.A. Sakkas, D.A. Lambropoulou, T.A. Albanis, *J. Photochem. Photobiol. A* 147 (2002) 135–141.
- [5] M. Kamiya, K. Kameyama, *Chemosphere* 45 (2001) 231–235.
- [6] A.D. Dimou, V.A. Sakkas, T.A. Albanis, *J. Photochem. Photobiol. A* 163 (2004) 473–480.
- [7] C. Catastini, M. Sarakha, G. Mailhot, *Int. J. Environ. Anal. Chem.* 82 (2002) 591–600.
- [8] A.D. Dimou, V.A. Sakkas, T.A. Albanis, *J. Agric. Food Chem.* 53 (2005) 694–701.
- [9] G. Durand, D. Barceló, J. Albaigés, M. Mansour, *Chromatographia* 29 (1990) 120–124.
- [10] N. de Bertrand, D. Barceló, *Anal. Chim. Acta* 254 (1991) 235–244.
- [11] V.A. Sakkas, D.A. Lambropoulou, T.A. Albanis, *Chemosphere* 48 (2002) 939–945.
- [12] S. Chiron, J. Abián, M. Ferrer, F. Sánchez-Baeza, A. Messeguer, D. Barceló, *Environ. Toxicol. Chem.* 14 (1995) 1287–1298.
- [13] L. Marcheterre, G.G. Choudhry, G.R.B. Webster, *Rev. Environ. Contam. Toxicol.* 103 (1988) 61–126.
- [14] G. Kopf, W. Schwack, *J. Pesticide Sci.* 43 (1995) 303–309.
- [15] G. Durand, D. Barceló, *J. Chromatogr.* 502 (1990) 275–286.
- [16] I. Ferrer, M. Mezcuca, M.J. Gómez, E.M. Thurman, A. Agüera, M.D. Hernando, A.R. Fernández-Alba, *Rapid Commun. Mass Spectrom.* 18 (2004) 443–450.
- [17] M. Ibáñez, J.V. Sancho, O.J. Pozo, F. Hernández, *Anal. Bioanal. Chem.* 384 (2006) 448–457.
- [18] P. Sandín-España, J.J. González-Blázquez, J.O. Magrans, J.M. García-Baudín, *Chromatographia* 55 (2002) 681–686.
- [19] P. Sandín-España, J.O. Magrans, J.M. García-Baudín, *Chromatographia* 62 (2005) 133–137.
- [20] P. Sandín-España, I. Santín, J.O. Magrans, J.L. Alonso-Prados, J.M. García-Baudín, *Agron. Sustain. Dev.* 25 (2005) 331–334.
- [21] Y. Hashimoto, K. Ishihara, Y. Soeda, *J. Pesticide Sci.* 4 (1979) 299–304.
- [22] Y. Soeda, K. Ishihara, I. Iwataki, H. Kamimura, *J. Pesticide Sci.* 4 (1979) 121–128.
- [23] S. Ono, H. Shiotani, K. Ishihara, M. Tokieda, Y. Soeda, *J. Pesticide Sci.* 9 (1984) 471–480.
- [24] S. Chiron, C. Minero, D. Vione, *Ann. Chim. Rome* 97 (2007) 135–139.
- [25] OECD Environmental Health and Safety Publication. OECD (Organisation for Economic Cooperation and Development). Guidance Document for Testing of Chemicals. Phototransformation of Chemicals in water—Direct and indirect photolysis, 2000.
- [26] M. Kamiya, K. Kameyama, *Chemosphere* 36 (1998) 2337–2344.
- [27] G.R. Helz, R.G. Zepp, D.G. Crosby (Eds.), *Aquatic and Surface Photochemistry*, Lewis Publishers, Boca Raton, 1994.
- [28] M. Elazzouzi, A. Bensaoud, A. Bouhaouss, S. Guittoneau, A. Dahchour, P. Meallier, A. Piccolo, *Fresenius Environ. Bull.* 8 (1999) 478–485.
- [29] A.D. Dimou, V.A. Sakkas, T.A. Albanis, *Int. J. Environ. Anal. Chem.* 84 (2004) 173–182.
- [30] P. Boule (Ed.), *The Handbook of Environmental Chemistry*, vol. II, Part L: Reactions and Processes: Environmental Photochemistry, Springer, 1999.
- [31] R. Andreozzi, M. Raffaele, P. Nicklas, *Chemosphere* 50 (2003) 1319–1330.
- [32] H. Chaabane, E. Vulliet, F. Joux, F. Lantoine, P. Conan, J.-F. Cooper, C.-M. Coste, *Water Res.* 41 (2007) 1781–1789.
- [33] P. Mazellier, J. Jirkovsky, M. Bolte, *J. Pesticide Sci.* 49 (1997) 259–267.
- [34] F. Galichet, G. Mailhot, F. Bonnemoy, J. Bohatier, M. Bolte, *Pesticide Manage. Sci.* 58 (2002) 707–712.
- [35] H. Park, W. Choi, *J. Photochem. Photobiol. A* 159 (2003) 241–247.
- [36] J.W. Kwon, K.L. Armbrust, *J. Pharm. Biomed. Anal.* 37 (2005) 643–648.
- [37] L.N. Falb, D.C. Bridges, A.E. Smith, *J. Agric. Food Chem.* 38 (1990) 875–878.
- [38] C. Kolano, G. Bucher, D. Grote, O. Schade, W. Sander, *J. Photochem. Photobiol.* 82 (2006) 332–338.
- [39] F. Amat-Guerri, R. Mallavia, R. Sastre, *J. Photopolym. Sci. Technol.* 8 (1995) 205–232.